Pharm Res (2015) 32:2503–2515
DOI 10.1007/s11095-015-1639-9

RESEARCH PAPER

Measurement of Shrinkage and Cracking in Lyophilized Amorphous Cakes. Part II: Kinetics

Sabine Ullrich • Stefan Seyferth • Geoffrey Lee

Received: 1 December 2014 / Accepted: 22 January 2015 / Published online: 6 February 2015

ABSTRACT

Purpose Measurement of the kinetic development of shrinkage and cracking of an amorphous trehalose cake as they take place during lyophilization.

Methods A novel technique has been developed which monitors a vial *in situ* during the freeze-drying cycle. The 2-dimensional degrees of shrinkage and cracking in its top surface are determined quantitatively using a digital camera and evaluated using AxioVision.

Results Shrinkage and cracking develop largely already during programmed primary drying and are coupled. For trehalose, sucrose and maltose no clear correlation between shrinkage and w_g' is found. There is no dependence of cake rim detachment from the vial inner surface on the trehalose concentration. Cake adhesion is therefore likely not the only determining factor for detachment and shrinkage.

Conclusions If shrinkage can occur during primary drying, then this relaxes the drying tension produced by desorption of non-frozen water out of the amorphous structure left behind as the sublimation front passes through a volume element, and causes little or no cracking. If shrinkage is restrained, then the drying tension is relaxed by cracking of the brittle cake.

KEY WORDS cake · cracking · lyophilization · morphology · shrinkage

ABBREVIATIONS

$t_{1\circ}$	% of programmed duration of primary drying.
$t_{2\circ}$	% of programmed duration of secondary drying.
T_g'	Glass transition temperature of maximally-freeze concentrated solution.
T_{prod}	Product temperature measured with thermocouple.
T_{shelf}	Shelf temperature in freeze dryer.
w_g'	Non-frozen water content at point of maximum freeze concentration.

S. Ullrich · S. Seyferth · G. Lee (✉)
Division of Pharmaceutics, Friedrich Alexander University Erlangen, Cauerstrasse 4, 91058 Erlangen, Germany
e-mail: geoff.lee@fau.de

INTRODUCTION

The phenomena of shrinkage and cracking can be frequently observed in amorphous freeze-dried cakes. Shrinkage involves detachment and retraction of the cake from the inner wall of the glass vial (1), whereas cracking is the formation of fracture flaws through the cake mass (2). These structural changes are not a consequence of microscopic collapse of the cake structure caused by exceeding the critical temperature of the product (3). They are rather macroscopic changes in the cake that appear to be caused by the drying tension (4) built up within a solid on loss of solvent, i.e. water.

In our first paper on this subject (2) we identified a consistent pattern of coupling between shrinkage and cracking measured in freeze-dried trehalose cakes. A high degree of shrinkage evidently relaxes drying tension in the cake and results in little cracking. If shrinkage is restrained by a high tensile strength of the cake, the result is more extensive cracking to relax drying tension. Additionally, the measured degrees of shrinkage of three amorphous disaccharides (trehalose, maltose and sucrose) were found to correlate weakly with their different contents of non-frozen water at maximal freeze-concentration, w_g', as had been proposed earlier by Rambhatla *et al.* (2). This suggests that drying tension is developed by evaporative loss of the non-frozen water from the amorphous solid phase. Since this process starts as soon as a porous structure has been formed after the sublimation front has moved through a given volume element of the cake (5,6), it is likely that cake shrinkage is initiated early on during drying. In this sense, primary and secondary drying are almost simultaneous processes.

We present in this paper a novel technique for observing and quantifying the development of shrinkage and cracking

during freeze-drying. The aim is to determine the time-points at which the linked processes of shrinkage and cracking start to occur, and then to follow the subsequent kinetics of shrinkage and cracking and their relation to the drying rate. The assessment technique uses a digital camera to record the 2 dimensional patterns of shrinkage and cracking of the cake's top surface, as we have developed previously (2). A single vial within the freeze dryer is monitored *in situ* during the freeze-drying cycle and the extents of shrinkage and cracking determined independently using AxioVision picture processing software. The result is a comprehensive picture of the kinetic development of the two processes as they take place within the vial *in situ* in the freeze dryer.

We selected trehalose as a model substance that forms a fully- amorphous cake on freeze-drying. First, we examine the effects of the starting concentration of the trehalose on the kinetic development of shrinkage and cracking. Secondly, the kinetic behavior of the trehalose is compared with that of maltose and sucrose, two other disaccharides of differing w_g'. The kinetic results obtained throw further light on the mechanisms of the two processes and help explain how they can be reduced in extent.

MATERIALS AND METHODS

Materials

Trehalose dihydrate, sucrose and maltose were all obtained from Sigma Aldrich (Steinheim, Germany) and used as received. Water was double-distilled from an all-glass apparatus.

Methods

Each fill solution was prepared by dissolving the particular disaccharide in water and filtering the solution through a 0.2 μm pore-diameter membrane filter (Sartorius RC, Sartorius, Göttingen, Germany). Aliquots of fill solution were then pipetted into 2R glass tubing vials (VC002-13c; Schott, Mülheim, Germany). An aliquot volume of 300 μL gave a fill height of approximately 2.5 mm. The neck region of this 'sample' vial had been removed by horizontal cutting to allow unobstructed observation of the cake's top surface from above. Filled vials were then placed on the middle-shelf of a Martin Christ (Osterhode am Harz, Germany) Delta 1–24 KD freeze dryer of total shelf area 0.31 m^2 in the arrangement shown in Fig. 1a. The machine was selected because the drying chamber has a transparent Plexiglas cover which allows continual observation of the vials in cross section from above (see description of camera technique below). The horizontal arrangement of the vials was around a freeze-drying microbalance (CWS-40, 2nd Edition; Martin Christ) situated on the same shelf. The sample vial was surrounded by one layer of neck-free, cut, filled vials which were situated within the hexagonal arrangement of regular uncut, filled vials. The top shelf of the freeze dryer was perforated at a position exactly above the sample vial on the shelf below it, as shown in Fig. 1b. This allowed camera observation of the sample vial through the transparent Plexglas cover of the freeze dryer from above. A thermocouple (T type, PTFE 36) was placed in one of the regular vials. Freeze drying was performed using a routine process cycle: $T_{shelf} = -40°C$ (2 h) with subsequent ramps to −20°C for primary drying (35 h) and 25°C for secondary drying (5 h); chamber pressure = 0.04 mbar. The drying rate during the freeze-drying cycle was determined using the microbalance (cf. Fig. 1a) that held a second neck-free, cut, filled vial. The procedure has been fully described before (7).

The camera system comprised an EOS 60D digital camera (Canon, Krefeld, Germany) with an EF 100 mm f2.8 USM macro lens (Canon) and a Siocore 48-LED macro ring light (Siocore, Lübeck, Germany) mounted on a tripod (Manfrotto 055XPROB; Cologne, Germany) above the freeze dryer's Plexiglas cover. The Plexiglas cover is completely blacked-out on its cylindrical sides. The macro ring light is placed directly in front of the macro lens using an adapter ring and ensures even, shadow-free illumination of the cake suface. The camera focus was set to the mid-point between the centre locus and the circumference of the cake's top surface. An ISO value of 800 gave low noise and good image quality. A monochrome image of the cake's top surface was taken every 10 min during the freeze drying cycle and stored as a RAW file.

High dynamic range (HDR) imaging (8) was used to balance fluctuations in image brightness and avoid loss of detail-resolution in excessively bright or dark areas of the cake surface. Three images of the cake top surface were taken each at a different exposure (auto exposure bracketing or AEB) set to −0.3, 0.7, or 1.7. The HDR final image was then formed by bracketing the three images using Digital Photo Professional software. The RAW file was then converted to TIFF or JPEG.

The extents of shrinkage and cracking were then determined using image evaluation (2). Briefly, *shrinkage* was quantified using AxioVision 4.8.2 (Carl Zeiss Vision, Aalen, Germany) to measure the cross-sectional inner area of the vial, A_v [$pixel^2$], and the cake top surface area, A_F [$pixel^2$]. The degree of shrinkage, S(t) [%], was calculated from:

$$S(t) = A_F \cdot 100 / A_v \quad (1)$$

Cracking was quantified by again measuring A_F with AxioVision, and the areas of cracking using Matlab (Mathworks, Natick, MA, USA) to determine the brightness of the pixels within A_F. To distinguish between areas of intact cake surface and areas of cracking, a threshold value of brightness was calculated for each cake from the mean brightness value of the intact cake area. The sum of all crack pixels gives the total

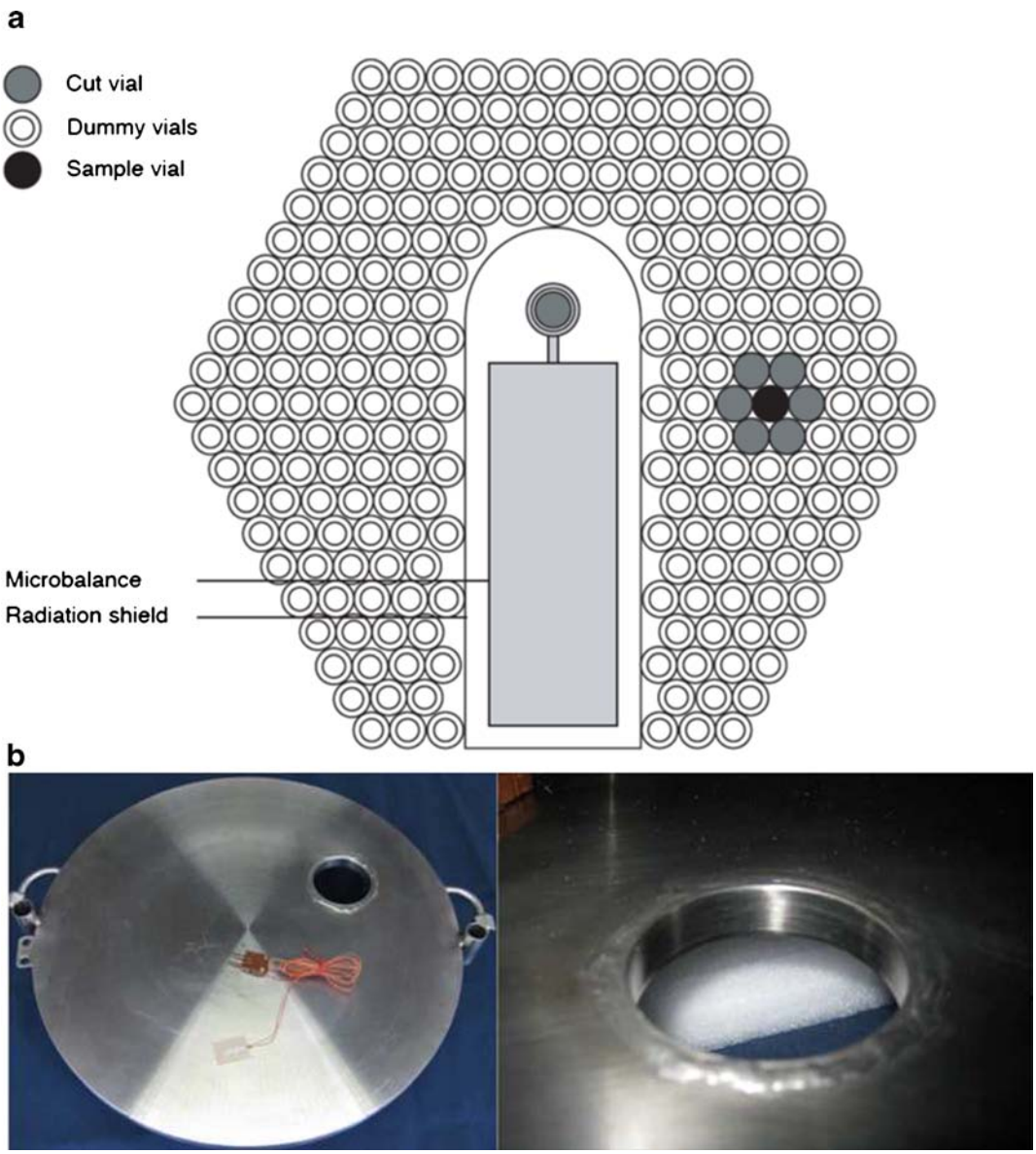

Fig. 1 Details of freeze drying process used. (**a**) Arrangement of cut 'sample' vial (*black*), cut vials (*dark grey*) and uncut 'dummy' vials (*light grey*) on shelf of freeze dryer. The vials are arranged around the microbalance holding one cut vial (*dark grey*). (**b**) Photographs of isolated top shelf of the freeze dryer to illustrate the perforation machined vertically above the position of the 'sample' vial standing on shelf below.

crack surface area, A_c [pixel^2]. The degree of cracking, C(t) [%], is then given by:

$$C(t) = A_c \cdot 100 / A_F \quad (2)$$

See reference (2) for full details.

RESULTS & DISCUSSION

10% *w/w* Trehalose

Figure 2 shows the result for freeze-drying a 10% *w*/*w* aqueous trehalose solution from three replicate runs (mean average value ± standard deviation). Note that the x-axis is partitioned into the primary drying and secondary drying phases whose programmed durations are 35 h and 5 h, respectively. The scale of the partitioned x-axis is given as % of the programmed duration of primary or secondary drying, $t_{1\circ}$ or $t_{2\circ}$. The two upper frames (Fig. 2a and b) show the kinetic development of cracking and shrinkage. The third frame from the top (Fig. 2c) shows the shelf and product temperatures. The lower frame (Fig. 3d) gives the results from the microbalance measurements and shows both the cumulative water loss and its first derivative equal to the drying rate.

At the start point of primary drying, i.e. $t_{1\circ}=0\%$, there is no detectable shrinkage or cracking of the

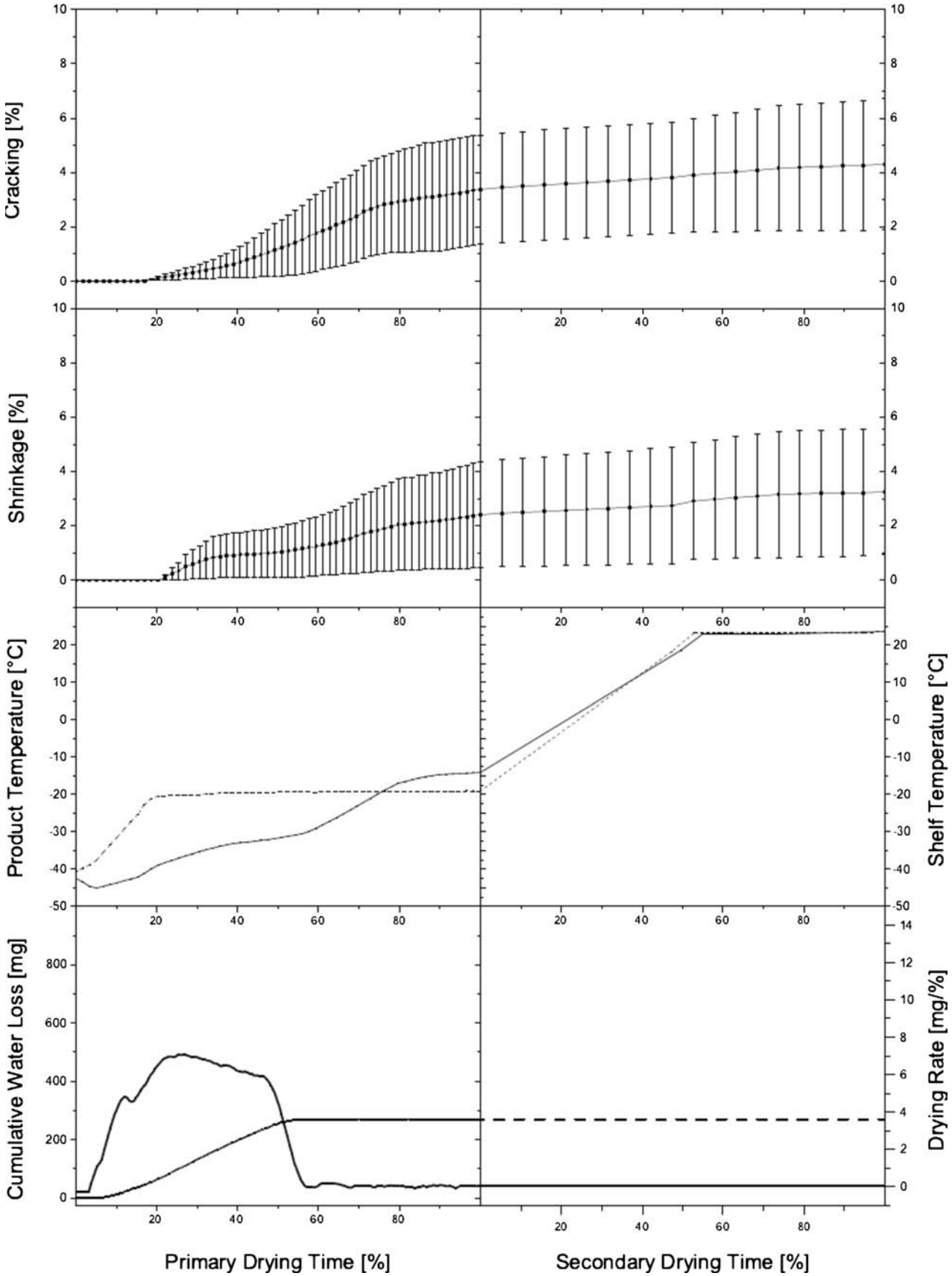
Cracking [%]
Shrinkage [%]
Product Temperature [°C]
Shelf Temperature [°C]
Cumulative Water Loss [mg]
Drying Rate [mg/%]
Primary Drying Time [%]
Secondary Drying Time [%]

◀ **Fig. 2** Freeze drying of 10% *w/w* trehalose in water. Top frame (**a**): kinetic development of extent of cracking; second from top frame (**b**): kinetic development of extent of shrinkage; third from top frame (**c**): product temperature, T_{prod}, (continuous line) measured with thermocouple in vial, and shelf temperature, T_{shelf} (*dotted line*); bottom frame (**d**): cumulative water loss [%] (dotted line) and drying rate [mg/%] (continuous line) as measured using microbalance. The values for cracking and shrinkage are the mean ± SD of $n = 3$ runs.

frozen cake (Fig. 2a & b). During the previous freezing step there will have been phase separation of ice from the aqueous trehalose solution (9). Water is removed from the increasingly-concentrated trehalose solution up to the point of maximum freeze-concentration at T_g' where the trehalose solution now forms a glassy state (5). The removal of water from a wet solid will produce a so-called drying tension within the solid (4). This is a tensile stress, which if not relaxed by shrinkage can lead to cracking of the solid (10). This is the typical behavior of forced-convection drying of a solid where the water is removed by evaporation from the solid/

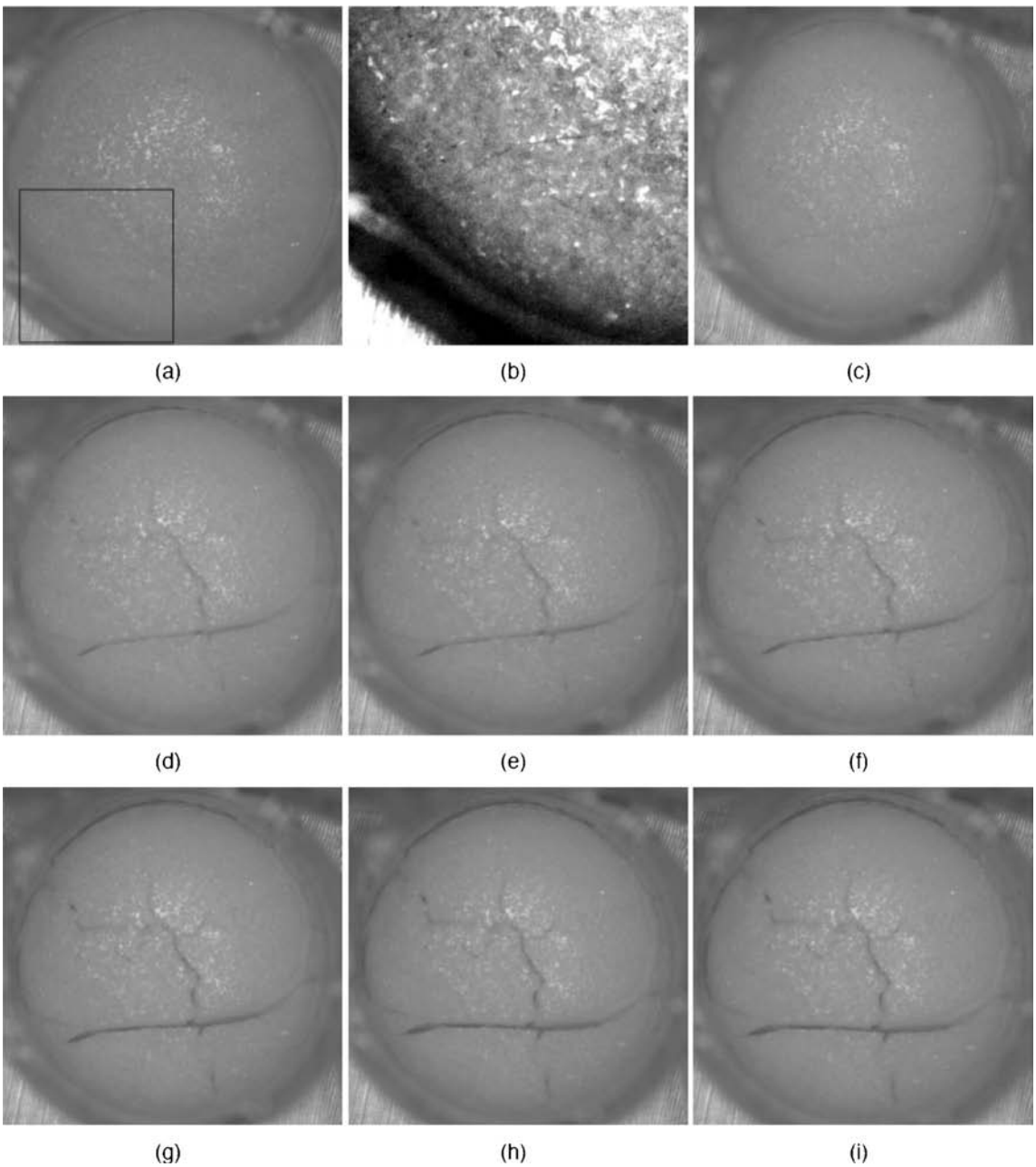

Fig. 3 Images of freeze drying of 10% *w/w* trehalose in water taken after different process durations of programmed primary (t_{1°) and secondary (t_{2°) drying. A) $t_{1^\circ} = 15\%$; b) magnification of a) to illustrate first crack appearance; c) $t_{1^\circ} = 40\%$; d) $t_{1^\circ} = 70\%$; e) $t_{1^\circ} = 75\%$; f) $t_{1^\circ} = 100\%$; g) $t_{2^\circ} = 40\%$; h) $t_{2^\circ} = 85\%$; i) $t_{2^\circ} = 100\%$. The images were taken from one run but are representative of all three runs.

gas interface (11). In the case of the freezing step of freeze-drying, the water is removed by phase separation from an increasingly-concentrated trehalose solution to form ice crystals first within the liquid solution which progressively turns into a glassy solid. The lack of shrinkage or cracking during the freezing step of lyophilization (cf. Fig. 2a & b at $t_{1\circ}=0\%$) means that the drying tension generated in the trehalose phase by phase separation of ice during freezing is relaxed because the increasingly freeze-concentrated trehalose solution is still a mobile fluid. Only as its viscosity increases strongly on approaching the glassy state at T_g' (12) will its mobility be reduced. Both the increased viscosity and the higher trehalose concentration (13) will hinder further ice crystal growth, and the result is the formation of a frozen cake without shrinkage or cracking of the glassy trehalose phase. The removal of water from a solution by freezing-induced phase separation avoids therefore formation of a cracked solid, in contrast to its removal by evaporative drying (10).

Both shrinkage and cracking start during the early stages of primary drying and are detected at $t_{1\circ}=20\%$. Figures 2b & a show that both increase continually and simultaneously during the subsequent course of primary drying. The camera image in Fig. 3c illustrates the area of initial shrinkage developing at the top left-hand edge of the cake surface where detachment of the circumference of the cake's top surface from the inside wall of the vial has occurred. After $t_{1\circ}=50\%$ this area of shrinkage becomes more and more visually evident (Fig. 3d-f) and the degree of shrinkage increases (Fig. 2b). At the same time there is a sharp decline in drying rate (Fig. 2d) and hence a rise in T_{prod} (Fig. 2c) well before the primary drying phase reaches its programmed end point at $t_{1\circ}=100\%$.

The shrinkage observed involves detachment of the circumference of the cake's top surface from the inside wall of the vial (visible in Fig. 3c at $t_{1\circ}=40\%$) followed by contraction of the cake mass. This means that T_{prod} must be high enough to allow plastic flow of the amorphous cake mass (1), at least in the periphery region of the cake. Indeed, after $t_{1\circ}=50\%$ the degree of shrinkage increases again after a short plateau phase (Fig. 2b) which correlates with the rise in T_{prod} after this time. Recall that T_{prod} is measured at the bottom center point of the vial base, whereas shrinkage take place in the peripheral regions of the cake (2). . T_{prod} will rise earlier in the periphery as the sublimation front first passes through these regions during drying. We suggest that the rise in T_{prod} in the peripheral regions of the amorphous structure left behind after the sublimation front has passed through a volume element allows detachment and cake contraction. Detachment clearly must precede any shrinkage.

The characteristic first sign of cracking is the appearance of a single hairline crack. Figure 3a shows a representative image of this behavior taken at $t_{1\circ}=15\%$ and Fig. 3b a magnification of the crack region. The calculated crack area is only 0.0009% at this time point and therefore not evident in the graph of Fig. 2a. Subsequently, the degree of cracking in Fig. 2a increases as further cracks appear and propagate in length (Fig. 3c). This behavior levels off at $t_{1\circ}=75\%$ (Fig. 2a), since after this time no new cracks appear nor further crack elongation takes place (Fig. 3e). For the remainder of programmed primary drying and the whole duration of programmed secondary drying the increase in cracking is slower (Fig. 2a) as only lateral expansion of the already existing cracks occurs (Fig. 3e–i). This is paralleled by the gradual increases in degree of shrinkage during the course of secondary drying. The gap between the cake's top surface circumference and the inner wall of the vial becomes larger in the region of detachment (Fig. 3g–i).

The detected end-point of primary drying is judged from consideration of both the product temperature, T_{prod}, and microbalance results. In Fig. 2c we observe that T_{prod} starts its sharp increase at approximately $t_{1\circ}=60\%$. At this time-point the drying-rate measured by the microbalance has already sharply declined since $t_{1\circ}=50\%$. The microbalance vial is expected to dry faster than the other vials because it is not part of the hexagonal array of filled vials and also experiences enhanced radiation heat transfer from the stainless steel cover of the microbalance (7). These two results mean that primary drying, i.e. local sublimation, is largely finished at $t_{1\circ}=60\%$ (5). Shrinkage and cracking have, however, already strongly progressed up to this time and reached 40% and 48% of their respective final values. Both processes subsequently accelerate between $t_{1\circ}=60\%$ and $t_{1\circ}=80\%$ (Fig. 2a & b) where T_{prod} reaches the shelf temperature, T_{shelf}. At $t_{1\circ}=80\%$ the degrees of shrinkage and cracking reach 71% and 78% of their respective final values. Shrinkage and cracking are seen therefore to be initiated and to develop strongly during the programmed primary drying stage. Both processes continue to develop during secondary drying, as Fig. 2a & b clearly show. This means that the design of the secondary drying cycle is relevant for shrinkage and cracking behavior. The pattern and extent of shrinkage and cracking are, however, established during primary drying. Note that the weight-loss recorded on the microbalance (Fig. 2d) decreases sharply between $t_{1\circ}=50\%$ and 60%, but falls to zero first at $t_{1\circ}\approx90\%$. Yet the microbalance results clearly show a break at $t_{1\circ}=50-60\%$, which is likely to be the end point of sublimation. The 2°C-overshoot of T_{prod}

Fig. 4 Comparison of freeze-drying of 5% *w/w* (*red*), 10% *w/w* (black) and 30% *w/w* (*blue*) trehalose in water. Top frame (**a**): kinetic development of extent of cracking; second from top frame (**b**): kinetic development of extent of shrinkage; third from top frame (**c**): product temperature, T_{prod}, measured with thermocouple in vial, and shelf temperature, T_{shelf}; bottom frame (**d**): cumulative water loss [%] and drying rate [mg/%] as measured using microbalance. The values for cracking and shrinkage are the mean ± SD of n = 3 runs.

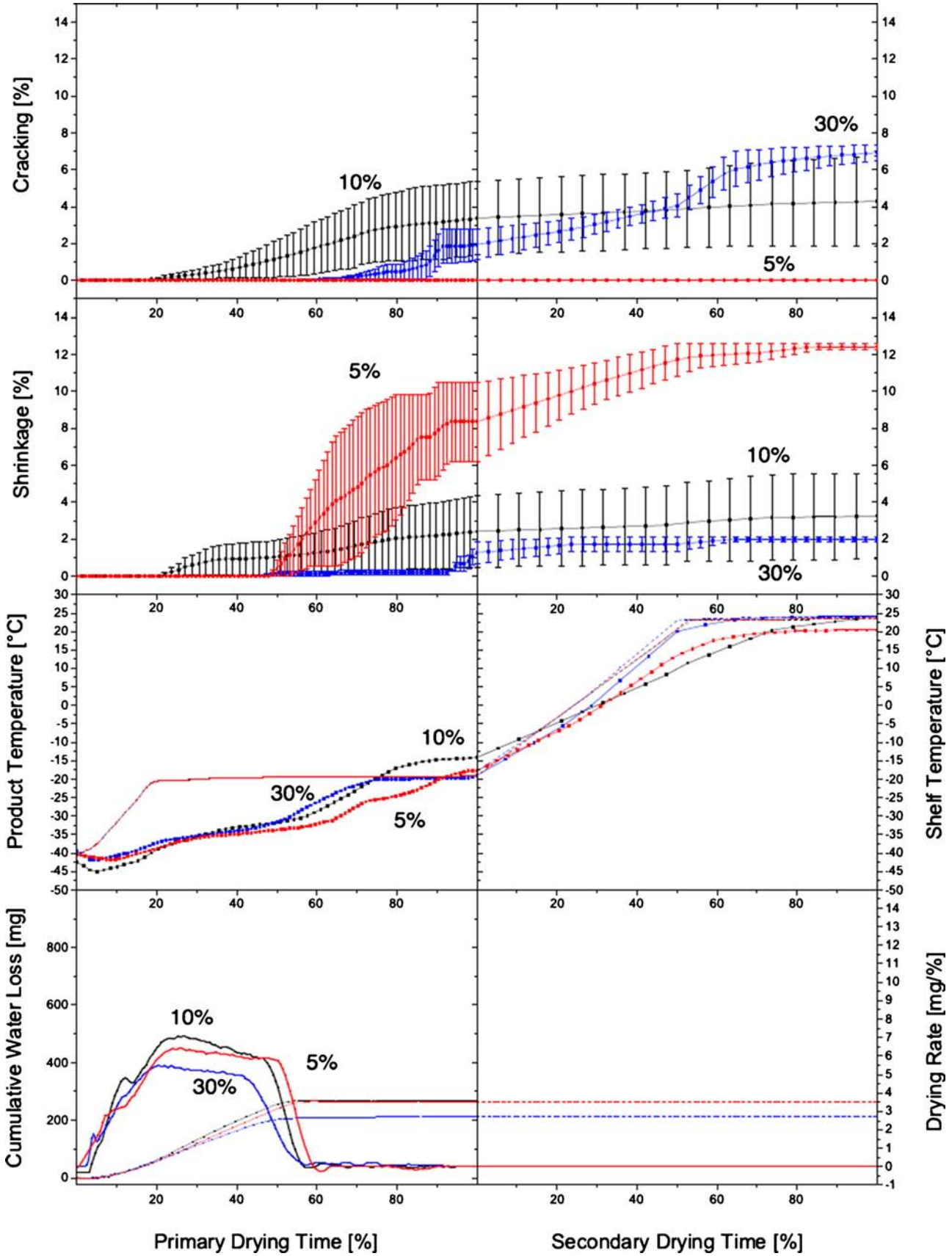
Cracking [%]
10%
30%
5%
Shrinkage [%]
5%
10%
30%
Product Temperature [°C]
10%
30%
5%
Shelf Temperature [°C]
Cumulative Water Loss [mg]
10%
5%
30%
Drying Rate [mg/%]
Primary Drying Time [%]
Secondary Drying Time [%]

through T_{shelf} is attributed to radiation heat transfer to the vial from the chamber wall (14).

The microbalance registers the start of loss of water at $t_{1\circ}$= 3% rising to a maximum rate of loss at $t_{1\circ}$=25% (Fig. 2d). The first appearance of cracking (still in the absence of shrinkage) is, however, monitored much later at $t_{1\circ}$=15% (Fig. 2a). After this time a large amount of water has already been lost from the cake – some 40 mg out of a total water loss during primary drying of 270 mg, mostly by sublimation (15). This large water loss before the first appearance of cracking indicates that sublimation is not the cause of cracking. The alternative explanation is that desorption of non-frozen water out of the porous, amorphous structure left behind after the sublimation front has passed through a volume element of the cake causes cracking. This desorption of water occurs by evaporation at the newly-formed solid/gas interface. This causes a build up of drying tension within the deeper regions of the still-wet solid that cannot be relaxed because of the glassy state. The result is brittle fracture and cracking (10).

These results thus show that shrinkage and cracking of a trehalose cake develop largely during the programmed primary drying phase. They further indicate that both phenomena occur in the amorphous cake structure left behind after l the sublimation front has passed through a volume element of the cake. Shrinkage is a result of rise in T_{prod} in the peripheral cake regions to allow plastic flow, and cracking a result of water desorption from the exposed solid/gas interface to produce drying stress. This pattern of behavior is a consequence of the near simultaneous occurance of primary and secondary drying, i.e. sublimation and evaporation. During programmed secondary drying the further development of cracking and shrinkage is much reduced. In this phase the microbalance registers no further water loss (Fig. 2d). This device has, in our experience, a reliable lower detection limit of 5 mg which is equal to 2% *w*/*w* of the trehalose cake mass (fill volume 2.5 g of a 10% *w*/*w* trehalose). This means that the residual water content at the end of primary drying was less than this figure, otherwise it would have been detected by the microbalance. If the frozen cake contained w_g' of 16.7% (16) at $t_{1\circ}$=0%, then the at-most 2% moisture removed during secondary drying results in the observed small increases in cracking or shrinkage. As Fig. 3f-i show, both the further cracking and shrinkage come from expansion of the already existing cracks and detachment areas. It follows that cracking and shrinkage during secondary drying will depend on the amount of residual water left in the cake at the end of primary drying.

Effects of Altering Trehalose Concentration

The kinetic pattern of cracking and shrinkage alters with change in concentration of trehalose in the fill solution. Consider first the extent of cracking. A reduction in trehalose concentration from 10% to 5% reduces the degree of measured cracking to zero at all times during the freeze-drying cycle (Fig. 4a). An increase in concentration from 10% to 30% delays the onset of cracking during programmed primary drying, but this subsequently develops strongly with secondary drying to give the highest degree of cracking in the end-product. The degree of cracking measured in the end-product is therefore directly proportional to trehalose concentration, which is consistent with our previous measurements on end-product vials using the dark cell (2). The values for cracking and shrinkage determined with the *in situ* technique are, however, lower than the corresponding values measured with the dark cell. This is just a result of the strong background light used in the dark cell which produces a much higher contrast between the light areas of the cracking/shrinkage voids and the darker areas of intact cake.

The coupling of cracking and shrinkage that has been demonstrated on end-product cakes (2) is also observed in these kinetic measurements. With 5% trehalose Fig. 4b shows how shrinkage starts at $t_{1\circ}$=50% and then develops very rapidly through the remainder of primary and all of secondary drying. The images illustrate a still intact cake at $t_{1\circ}$=40% (Fig. 5a) which changes to complete cake detachment and uniform shrinkage at $t_{1\circ}$=48% (Fig. 5b). A further uniform shrinkage is observed up to the end of secondary drying (Fig. 5c–f). This rapid development of shrinkage is associated with a lack of cracking in any of the images in Fig. 5. As the trehalose concentration is increased through 10% up to 30% the degree of shrinkage declines (Fig. 4b) and cracking increases (Fig. 4a). This is illustrated by the images from the 30% trehalose cakes in Fig. 6 where the development of cracking is particularly evident. The sharp further increase in degree of cracking towards the end of secondary drying (Fig. 4a) is seen to be a result of lateral expansion of the already existing cracks (Fig. 6e and f). This is consistent with the behavior of the 10% trehalose cakes discussed above.

The inverse coupling between shrinkage and cracking is therefore already largely, but not fully, developed during primary drying. If the drying tension that is produced by desorption of non-frozen water out of the amorphous structure left behind as the sublimation front passes through a volume element of the cake can be relaxed by shrinkage, then little cracking occurs. This is the behavior seen with the 5% trehalose fill solution. The constraining of shrinkage at the higher trehalose concentrations of 10% and 30% results in more extensive cracking to relax the drying tension. Shrinkage and cracking taken place almost simultaneously because of the near simultaneous occurance of primary and secondary drying, i.e. sublimation and evaporation.

The reduction in shrinkage at higher trehalose concentration has already been observed in end-product cakes (2). The result in Fig. 4b shows that this dependence of shrinkage on trehalose concentration is manifest right from the point of

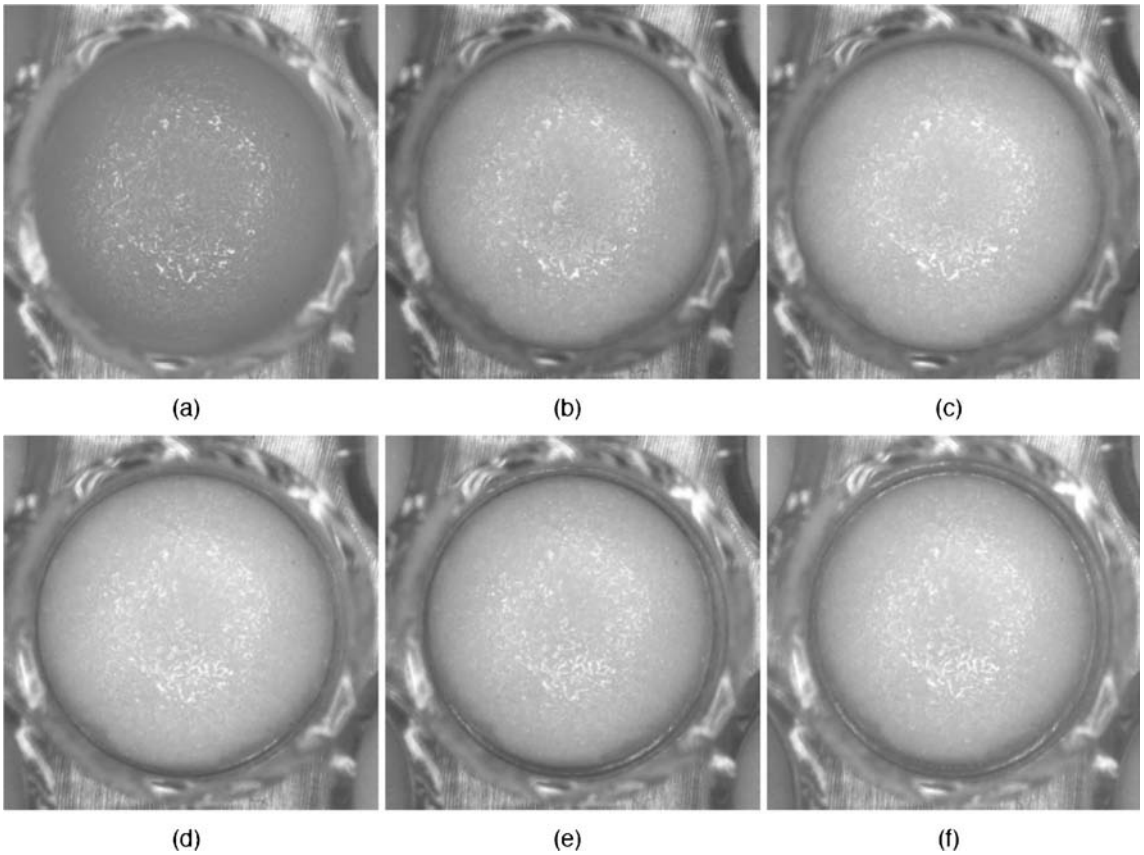

Fig. 5 Images of freeze-drying of 5% *w/w* trehalose in water taken after different process durations of programmed primary ($t_{1\circ}$) and secondary ($t_{2\circ}$) drying. (**a**) $t_{1\circ} = 40\%$; b) $t_{1\circ} = 48\%$; (**c**) $t_{1\circ} = 64\%$; (**d**) $t_{1\circ} = 88\%$; (**e**) $t_{1\circ} = 100\%$; (**f**) $t_{2\circ} = 100$. The images were taken from one run but are representative of all three runs.

onset of shrinkage during primary drying. The development of shrinkage is rapid and very strong at the lowest trehalose concentration of 5%, but is slower and weaker at the higher trehalose concentrations of 10% and 30%. The trehalose concentration has therefore a strong influence on the kinetics of shrinkage behavior. The point of onset of shrinkage is the time-point where detachment of the cake circumference from the inside wall of the vial is first detected during primary drying. This time-point is readily observed in Fig. 4b and lies at $t_{1\circ} = 50\%$ with both 5% and 30% trehalose concentrations and at $t_{1\circ} = 20\%$ with 10% trehalose. The trehalose concentration does not therefore determine cake detachment behavior, although it strongly influences subsequent shrinkage behavior. This finding puts into question the role played by adhesion of the cake to the inside wall of the vial for detachment. Intuitively, adhesion must play some role in detachment and hence shrinkage, but is probably only one of a number of determining factors. We suggest that other factors include the requirement of generating a local porous structure in the peripheral regions of the frozen cake before plastic flow can take place. This porous structure is provided by local sublimation of the ice crystals in the cake periphery, which explains the time-lag observed between the start of primary drying and the point of onset of detachment. This length of this time-lag is not dependent on trehalose concentration, possibly because the large mass of ice present outweighs any influence of the trehalose concentration in the range of up to 30% examined here. A further determining factor may be the increase in local T_{prod} in the periphery of the frozen trehalose phase towards T_g'. This occurs during primary drying and is necessary to promote the plastic flow (1) that initiates detachment of the cake circumference from the vial's inner wall. Figure 4c shows that at each trehalose concentration T_{prod} has risen from T_{shelf} by some 5°C by the time the point of onset of detachment has been reached. The values of T_{prod} reached at the onset of detachment are still well below T_g' of - 31°C (17), but the thermocouple is positioned at the vial bottom center. Shrinkage occurs primarily in the peripheral cake regions (2) where sublimation will have advanced more. T_{prod} (periphery) will therefore be higher and closer to T_g' at the point of onset of detachment than the thermocouple result in Fig. 4c suggests. There is, however, no clear correlation between T_{prod} (bottom center) and trehalose concentration in Fig. 4c either at the time point of detachment or later during shrinkage. Another determining factor appears to be the mechanical strength of the cake. With increasing trehalose concentration the tensile

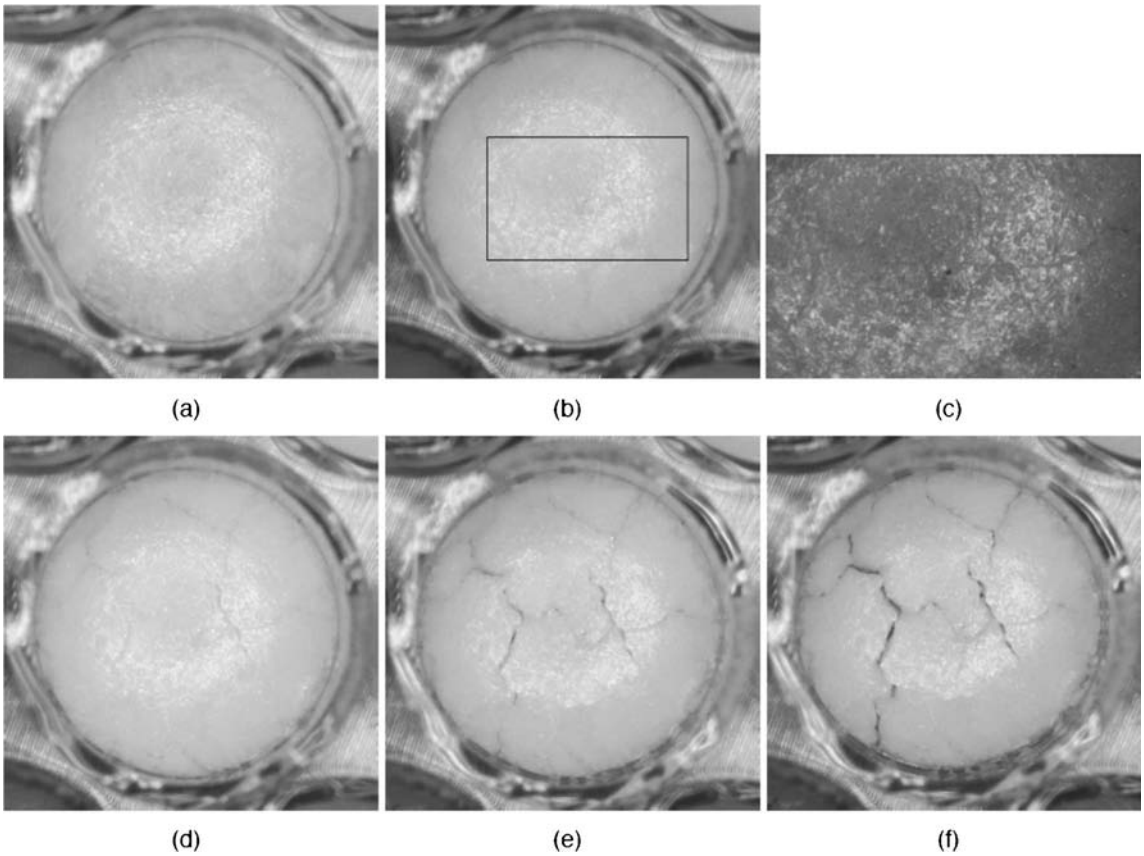

Fig. 6 Images of freeze-drying of 30% *w/w* trehalose in water taken after different process durations of programmed primary ($t_{1\circ}$) and secondary ($t_{2\circ}$) drying. (**a**) $t_{1\circ}$ = 15%; b) $t_{1\circ}$ = 60%; (**c**) magnification of (**b**) to illustrate crack appearance; (**d**) $t_{1\circ}$ = 90%; e) $t_{1\circ}$ = 100%; f) $t_{2\circ}$ = 100. The images were taken from one run but are representative of all three runs.

strength of the end-product cakes increases greatly and they also become more brittle (2). A correlation exists therefore between reduced shrinkage and greater cake hardness as trehalose concentration increases. This factor may outweight the influence of the other factors adhesion, pore formation, and T_{prod} in determining the strong effect of trehalose concentration on shrinkage in Fig. 4b.

Comparison of Sucrose, Maltose and Trehalose

The previous study using the dark cell on final-product cakes (2) failed to show that the degrees of shrinkage of the 3 disaccharides trehalose, maltose and sucrose were in sequence with their different values of w_g' (N.B. w_g' for sucrose is approximately 18.5% (16)), as had been proposed earlier by Rambhatla *et al.* (1). Figure 7b shows the kinetics of shrinkage in these same three disaccharides. The shrinkages at $t_{2\circ}$ = 100% also do not correlate with the sequence of values of w_g': maltose with w_g' of 20.0% (18) has shrinkage of 8.4%; sucrose with w_g' of 18.5% (16) has 10.1% shrinkage; and trehalose with w_g' of 16.7% (17) has shrinkage of 5.3%. It may be that the values of w_g' are too close to distinguish between differences in shrinkage.

The kinetic results show how shrinkage develops largely during primary drying up to these final-product values. Shrinkage starts to diverge between the 3 disaccharides at around $t_{1\circ}$ = 30%, with sucrose and maltose rising away from trehalose and reach substantially higher values at $t_{1\circ}$ = 100%. This suggests that sucrose and maltose can undergo more extensive plastic flow, possibly because of their slightly higher w_g'. Additionally, the maltose's T_{prod} (Fig. 7c) is markedly elevated during all of primary drying, although it drying rate is not lower than with the other two disaccharides (Fig. 7d). The sequence of final-product shrinkages of the three disaccharides is therefore already established by the end of primary drying. This gives credence to the idea that shrinkage is linked with the amount of unfrozen water lost from the amorphous phase during primary drying

Fig. 7 Comparison of freeze-drying of sucrose (*blue*), maltose (*red*) and ▶ trehalose (*black*), each 10% *w/w* in water. Top frame (**a**): kinetic development of extent of cracking; second from top frame (**b**): kinetic development of extent of shrinkage; third from top frame (**c**): product temperature, T_{prod}, measured with thermocouple in vial, and shelf temperature, T_{shelf}; bottom frame (**d**): cumulative water loss [%] and drying rate [mg/%] as measured using microbalance. The values for cracking and shrinkage are the mean ± SD of n = 3 runs.

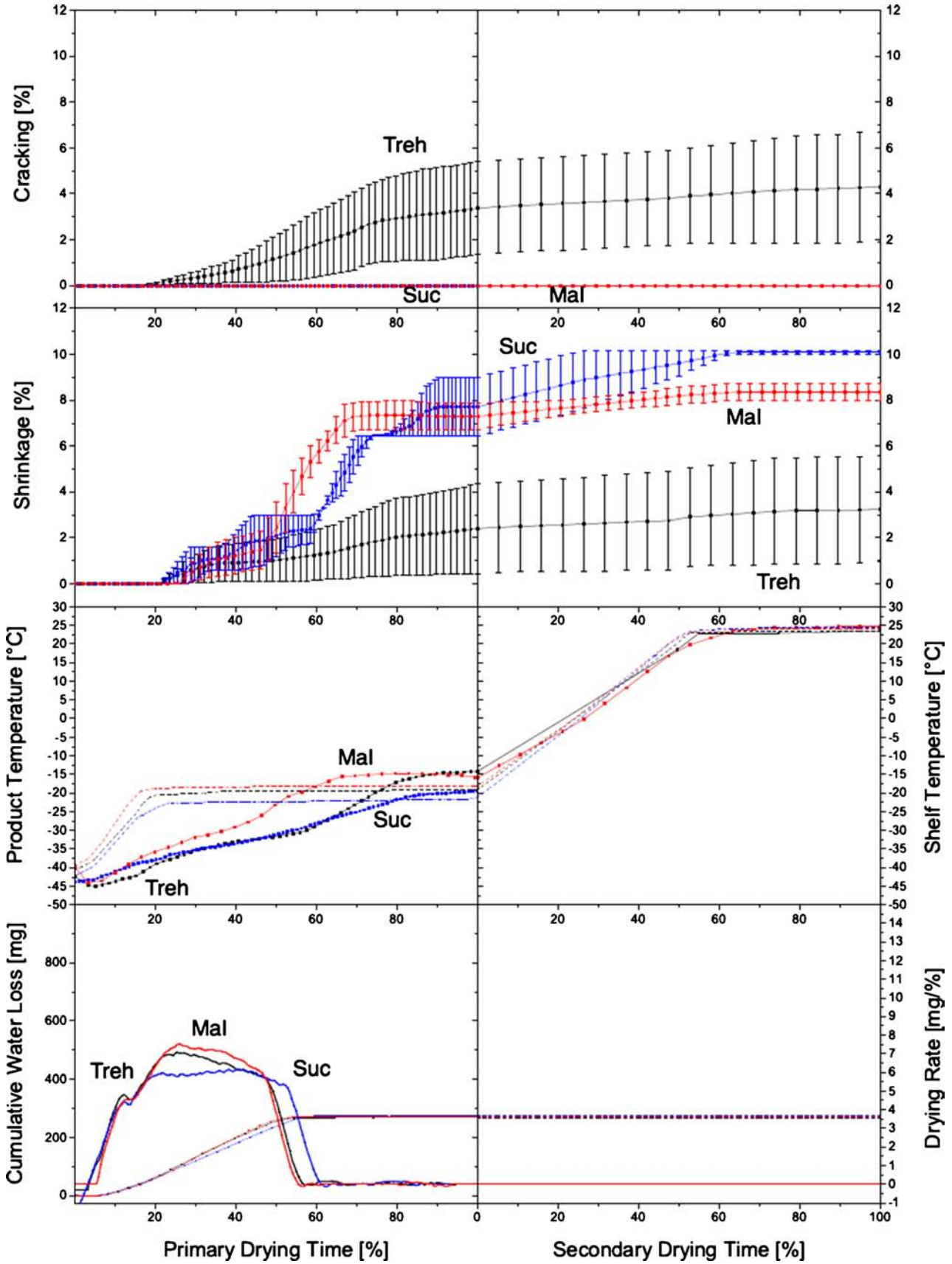
Cracking [%]
Treh
Suc
Mal
Shrinkage [%]
Suc
Mal
Treh
Product Temperature [°C]
Mal
Suc
Treh
Shelf Temperature [°C]
Cumulative Water Loss [mg]
Mal
Treh
Suc
Drying Rate [mg/%]
Primary Drying Time [%]
Secondary Drying Time [%]

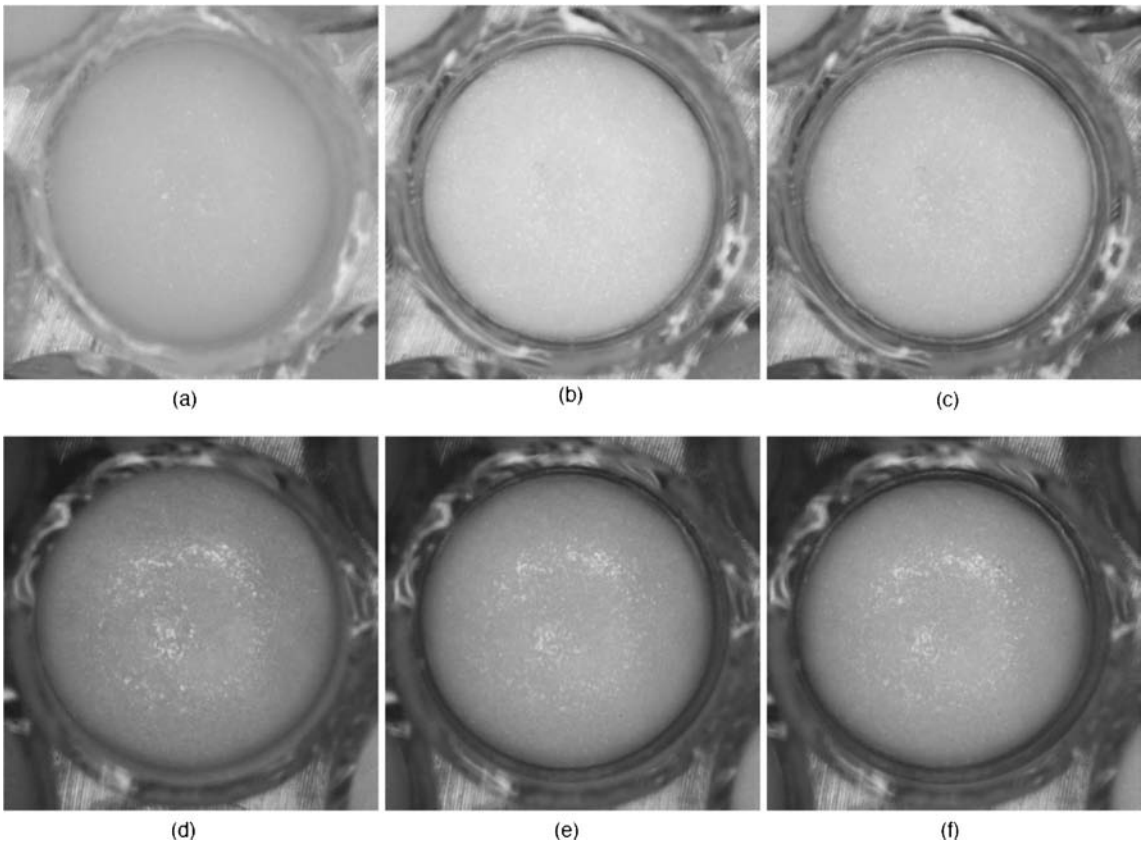

Fig. 8 Images of freeze-drying of different disaccharides, 10% *w/w* in water, taken after different process durations of programmed primary ($t_{1°}$) and secondary ($t_{2°}$) drying. (**a**) maltose, $t_{1°} = 0\%$; (**b**) maltose, $t_{1°} = 100\%$; (**c**) maltose, $t_{2°} = 100$; (**d**) sucrose, $t_{1°} = 0\%$; (**e**) sucrose, $t_{1°} = 100\%$; (**f**) sucrose, $t_{2°} = 100$. The corresponding images for trehalose are given in Fig. 3f and i for $t_{1°} = 100\%$ and $t_{2°} = 100\%$. All images were taken from one run but are representative of all three runs.

after local sublimation has created a solid/gas interface. The direct link to w_g' is, however, still missing.

The maltose and sucrose cakes develop no cracks during the whole of the freeze-drying cycle (Fig. 7). The images in Fig. 8 illustrate the appearance of detachment and shrinkage by the end of primary drying, but the complete lack of cracking. The high degrees of shrinkage relaxe the drying tension produced by desorption of non-frozen water out of the amorphous structure left behind as the sublimation front passes through a volume element of the cake sufficiently to avoid the necessity of cracking.

CONCLUSIONS

These kinetic measurements of shrinkage and cracking demonstrate the following behavior for the freeze-drying of aqueous trehalose:

1) Shrinkage and cracking are initiated and develop largely during the primary drying step. Both phenomena occur in the porous amorphous cake structure left behind as the sublimation front passes through a volume element of the cake. Shrinkage is therefore likely a result of rise in T_{prod} in the peripheral porous cake regions to allow plastic flow, and cracking a result of water desorption from the exposed solid/gas interface to produce drying stress.
2) Shrinkage and cracking are coupled. If shrinkage can occur, then this relaxes the drying tension produced by desorption of non-frozen water out of the amorphous structure left behind after local sublimation, and causes little or no cracking. If shrinkage is restrained, then the drying tension is relaxed by cracking of the brittle cake.
3) Both shrinkage and cracking continue to develop during secondary drying, illustrating that the design of the secondary drying cycle is relevant. The pattern and extent of shrinkage and cracking are, however, established during primary drying.
4) No corelation between the point of onset of cake detachment from the vial wall and the trehalose concentration is found. This suggests that cake adhesion to the inside wall of the vial is not the only determining factor for shrinkage. Also relevant are the conditions in the cake periphery, i.e. formation of porosity as the sublimation front passes through a volume element, T_{prod} (periphery) and tensile strength.

ACKNOWLEDGMENTS AND DISCLOSURES

We recognize with thanks the comments of the two anonymous reviewers, which allowed us to improve the conclusions drawn from our work.

REFERENCES

1. Rambhatla S, Obert J, Luthra S, Bhuga C, Pikal M. Cake shrinkage during freeze-drying: a combined experimental and theoretical study. Pharm Devel Technol. 2005;1:33–40.
2. Ulrich S, Seyferth S, Lee G. Measurement of shrinkage and cracking in lyophilized amorphous cakes. Part I: final-product assessment. J Pharm Sci. 2015;104:155–74.
3. Johnson R, Oldroyd M, Ahmed S, Gieseler H, Lewis L. Use of monomeric temperature measurements (MTM) to characterize the freeze-drying behavior of amorphous protein formulations. J Pharm Sci. 2010;99:2863–73.
4. Kowalski S, Rajewska K. Drying-induced stresses in elastic and viscoelastic saturated material. Chem EngSci. 2002;57:3883–92.
5. Patel S, Doen T, Pikal M. Determination of end point of primary drying in freeze-drying process control. AAPS PharmSciTech. 2009;11:73–84.
6. Pikal M, Shah S, Roy M, Putman R. The secondary drying stage of freeze drying: drying kinetics as a function of temperature and chamber pressure. Int J Pharm. 1990;60:203–17.
7. Roth C, Winter G, Lee G. Continuous measurement of drying rate of crystalline and amorphous systems during freeze drying using an in situ microalance technique. J Pharm Sci. 2001;90:1345–55.
8. Reinhard E, Ward G, Pattanaik S, Debevec P, Heidrich W, Myszkowski K. High dynamic range imaging. 2nd ed. Burlingham: Morgan Kaufmann Publishers; 2010.
9. Franks F. Biophysics and biochemistry at low temperatures. Cambridge: Cambridge University Press; 1985.
10. Scherer G. Theory of drying. J Am Ceram Soc. 1990;73:3–14.
11. Lee W, Routh A. Why do drying films crack? Langmuir. 2004;20:9885–8.
12. Levine H, Slade L. Thermomechanical properties of small-carbohydrate-water glasses ansd ‚rubbers'. Kinetically metastable systems at sub-zero temperatures. J Chem Soc Farad Trans I. 1988;84:2619–33.
13. Uchida T, Nagayama M, Gohara K. Trehalose solution viscosity at low temperatures measured by dynamic light scattering method: trehalose depresses molecular transportation for ice crystal growth. J Crystal Growth. 2009;311:4747–52.
14. Patel S, Pikal M. Emerging freeze-drying process development and scale-up issues. AAPS PharmSciTech. 2011;12:372–8.
15. Tang X, Pikal M. Design of freeze-drying processes for pharmaceuticals: practical advice. Pharm Res. 2004;21(2):191–200.
16. Chang L, Milton N, Rigsbee D, Mishra D, Tang C, Thomas L, *et al.* Using modulated DSC to investigate the origin of multiple thermal transitions in frozen 10% sucrose solutions. Thermochim Acta. 2006;444(2):141–7.
17. Pyne A, Surana R, Suryanarayanan R. Enthalpic relaxation in frozen aqueous trehalose solutions. Thermochim Acta. 2003;405(2):225–34.
18. Hatley R, Franks F. Applications of DSC in the development of improved freeze drying processes for labile biologicals. J Therm Analy. 1991;37:1905–14.